Wide Power Range RF Energy Harvester for Powering Ultralow-Power Devices

Jesus Argote-Aguilar, Muh-Dey Wei, Florin-Doru Hutu, Guillaume Villemaud, Matthieu Gautier, Olivier Berder, Renato Negra

Wide Power Range RF Energy Harvester for Powering Ultralow Power Devices

Jesus Argote-Aguilar, *Student Member, IEEE,* Muh-Dey Wei, Florin-Doru Hutu, *Senior Member, IEEE,* Guillaume Villemaud, *Senior Member, IEEE,* Matthieu Gautier, Olivier Berder, *Member, IEEE,* and Renato Negra

***Abstract*—Harvesting Radio Frequency (RF) energy is an attractive solution for powering ultralow power devices. However, harvesting efficiently from different RF power levels is still a challenge. This work presents a wide power range RF harvester composed of a rectifier circuit and a Power Management Integrated Circuit (PMIC). Such a wide range is achieved by associating two independent rectifiers in parallel, one specifically optimized for low RF powers. In the association, the inductive matching technique is employed in each rectifier. It consists of an inductive branch comprised of a lumped inductor and a short-circuited stub whose values are selected to minimize ohmic losses. The operation range is controlled via the inductive branch values and by following the optimal load of the rectifier circuit with the PMIC, based on the input power level. The harvester is designed at 889 MHz and manufactured by using off-the-shelf components. Measured efficiencies of 29 % and 63 % are obtained at −20 dBm and 0 dBm, respectively, demonstrating the wide power range with high efficiency at low powers. At −20 dBm, the rectifier association keeps the PMIC active and delivers hundreds of nW at a regulated voltage of 1.8 V, which is suitable for ultralow power devices.**

***Index Terms*—Radio frequency (RF) energy harvesting, wireless power transfer (WPT), schottky rectifier, wide dynamic range, power management integrated circuit, ultralow power device.**

I. Introduction

In the context of an increasing deployment of the Internet of Things (IoT), the long-term operation of connected devices is limited by their batteries which, in most cases, is the classical power supply. The use of Wake-up Radio receivers (WuRx), driving the radio interface of the IoT on-demand, reduces the required energy since, most of the time, the main node is in a deep sleep state [1]. Moreover, making the WuRx independent of the main battery and powering it with harvested Radio Frequency (RF) energy will extend the battery lifetime of connected devices [2].

This paper is an expanded version from the International Workshop on Nonlinear Microwave and Millimetre-Wave Circuits, Aveiro, Portugal, November 8-10, 2023.

This work was supported by the COST ACTION CA20120 INTERACT.

This work is part of the project U-Wake funded by the French National Research Agency (ANR-20-CE24-0005).

Jesus Argote-Aguilar, Matthieu Gautier and Olivier Berder are with Univ Rennes, CNRS, IRISA, 35042 Rennes, France. (e-mail: name.surname@irisa.fr)

Florin-Doru Hutu and Guillaume Villemaud are with INSA Lyon, Inria, CITI, UR3720, 69621 Villeurbanne, France. (e-mail: name.surname@insa-lyon.fr)

Muh-Dey Wei and Renato Negra are with Chair of High Frequency Electronics, RWTH Aachen University, 52074 Aachen. (e-mail: name.surname@hfe.rwth-aachen.de)

With the advance of Ultralow Power (ULP) consumption electronic devices, ULP WuRx are now available. Powering them with energy harvested from low levels of the RF field is an interesting solution being investigated. Examples of ULP WuRx are [3] and [4], which have a power consumption in the order of nW.

This work proposes both powering ULP devices from low levels of the RF field and efficiently storing RF energy when higher RF power levels are available. Moreover, providing a regulated DC voltage, which is often required, is also considered. An RF rectifier provides the DC voltage, which is then managed and regulated by a Power Management Integrated Circuit (PMIC). The discussion is centered on the RF rectifier and divided into two main axes: (i) increasing its efficiency at low RF powers and (ii) extending its dynamic range.

Regarding harvesting at low power levels, as power decreases, the efficiency of the RF rectifier circuit also decreases due to ohmic losses brought by components. The performance of RF rectifiers is evaluated by the total efficiency η_T. This efficiency is defined as the ratio between the output DC power and the power provided by the RF source. It depends on the rectification efficiency η_{rect}, as well as the efficiency of the Matching Network (MN), η_{MN}, which encompasses both the capability of matching and the ohmic losses brought by its components. Different technologies and strategies are adopted to increase η_T. In CMOS standard technology, fully cross-coupled (FX) topologies reduce forward voltage drop losses in diode-connected transistors. This approach results in good η_{rect} [5]. Rectifiers based on Schottky diodes with low forward voltage drop losses also achieve high η_{rect} at low levels of the RF field [6]. Schottky diodes offer faster and less expensive implementation of prototypes. Another strategy to increase η_{rect} is the use of high Peak-to-Average Power Ratio (PAPR) signals as described in [7]–[9]. However, it leads to complex waveform design, reducing power amplifier efficiency on the transmitter side.

About extending the RF harvesting range, it is crucial to understand that RF rectifiers are power-dependent and typically optimized for specific input power levels. As the power level deviates from the expected value, there is a performance degradation. Different techniques have been proposed to extend the dynamic range. In typical diode-based topologies, good η_{rect} is achieved by following the rectifier optimal load based on the RF power level. The track of the optimal load is commonly achieved with DC/DC converters as proposed in [10] and [11]. Achieving a high η_T relies both on η_{rect} and on achieving

good matching across the desired dynamic range. In [12]–[19], combinations of Schottky diode-based rectifiers achieve a wide dynamic range by employing different techniques to match specific rectifiers in the combination according to the input RF power level. However, specific loads are used for each rectifier; alternatively, the rectifier is connected to a fixed voltage source, emulating a battery to be charged [20]. Furthermore, due to complex matching techniques introducing ohmic losses, efficiencies at low powers, such as -20 dBm, are very low or null.

The challenge addressed in the current study is the design of an efficient wide power range RF harvester providing a regulated DC voltage for a single device and starting to operate at power levels as low as -20 dBm.

The present work is an extension of the efficient low input RF power rectifier presented in [21], where the inductive technique is employed to reduce the complexity and losses of the MN by compensating the capacitive behavior of the diode with an inductive branch. Here, the wide RF rectifier circuit is achieved by the association in parallel of the efficient low input power RF rectifier with a rectifier for higher levels of the RF field. The inductive matching technique is employed in each rectifier of the association that results in a simple design using few components. Moreover, an original approach, which consists of a trade-off between the rectifier optimal load for η_{rect} and a load allowing a simpler MN with high η_{MN}, is discussed.

The RF power range is controlled with the inductive branches and by following the rectifier η_T optimal load with a Power Management Integrated Circuit (PMIC), based on the input power level. In addition to providing a maximum power point tracking (MPPT) algorithm, the PMIC also offers energy management and the regulation of the DC output voltage to a constant level. Interface requirements between our proposed rectifier circuit and a commercial PMIC are presented for reducing the quiescent power of the latter.

The main contributions of the present work are:

- Extending the dynamic range while keeping good efficiency at low powers by employing the inductive technique.
- The trade-off between the optimal load for η_{rect} and a load for an efficient impedance matching.
- Increasing the harvesting efficiency over a wide power range by optimizing η_{rect} conjointly with η_{MN}.
- Providing a regulated DC voltage from low RF field levels and efficiently storing energy across a wide range of RF power levels.

The RF harvester is designed at 889 MHz. By varying the inductive branch values, the operation frequency can be optimized to 868 MHz, or 915 MHz, which are commonly employed industrial, scientific, and medical (ISM) frequencies.

The paper is organized as follows: Section II describes in detail the design considerations of the low input power RF harvester, Section III discusses the design of the wide range RF harvester with performance starting at low powers, and Section IV concludes this paper.

II. Low input power RF harvester design

The RF harvester is composed of an RF rectifier followed by a PMIC, which regulates the output DC voltage of the rectifier. From the work initiated in [21] where the inductive matching technique is employed to design an efficient low input power rectifier, in this paper, this technique is presented in more detail and considerations on optimal choices for both components and rectifier topology are given in Section II-A. Interface considerations between the rectifier and the PMIC are given in Section II-B.

A. RF rectifier design

Having as the main target to harvest from low levels of the RF field and considering that the PMIC requires a minimum power and voltage delivered by the RF rectifier, the selection of the diode and rectifier topology is mainly decided at -20 dBm. To determine the suitable diode and rectifier topology, harmonic balance simulations are carried out by Keysight ADS software using standard Schottky equations. Fig. 1 compares η_{rect} of three Schottky diodes [22]–[24] and three typical diode-based topologies, *i.e.*, the series, the shunt, and the voltage doubler obtained at -20 dBm and 889 MHz.

The considered diodes have a low threshold voltage V_{th} leading to low forward voltage drop losses. Among the three considered diodes, the BAT15 from Infineon Technologies® achieves the highest efficiencies. This is explained by its low R_s limiting ohmic losses. The BAT17 diode also has a low R_s, whereas its higher C_{j0} along with R_s acts as a low-pass filter, attenuating the received RF signal to be rectified. Regarding the topology, the series and the shunt one-diode rectifiers have slightly higher efficiencies than the voltage doubler, which is a topology using at least two diodes. Effectively, the losses introduced by the forward voltage drop in diodes are significant at -20 dBm. As a result, the BAT15 diode in a single-diode topology is chosen. Moreover, the BAT15 diode reaches high efficiency at increased voltages due to higher DC values, which is suitable for the PMIC. It is worth mentioning that the parasitic inductance and capacitor of the package do not have an impact on η_{rect} under this efficiency definition. However, they must be considered when designing the MN.

As highlighted in Section I, at low powers, losses in the MN are critical. To reduce ohmic loss in complex MN as much as possible, the inductive matching technique [25] is used in the shunt topology along with the BAT15 diode. This technique uses an inductive branch L_b, in series with the diode, to compensate for its capacitive behavior as depicted in Fig. 2.

Considering the RF choke as ideal and neglecting R_s, the input impedance of the rectifier, Z_{in}, can be expressed as a function of the junction resistance $R_j(v)$, the junction capacitance $C_j(v)$ and L_b:

$$\Re(Z_{in}) = \frac{R_j(v)}{R_j^2(v)\omega^2\left[(C_j^2(v) + 2C_j(v)C_p + C_p^2\right] + 1}, \quad (1)$$

$$\Im(Z_{in}) = (L_b + L_p)\omega + R_j(v)\omega\left[C_j(v) + C_p\right]\Re(Z_{in}). \quad (2)$$

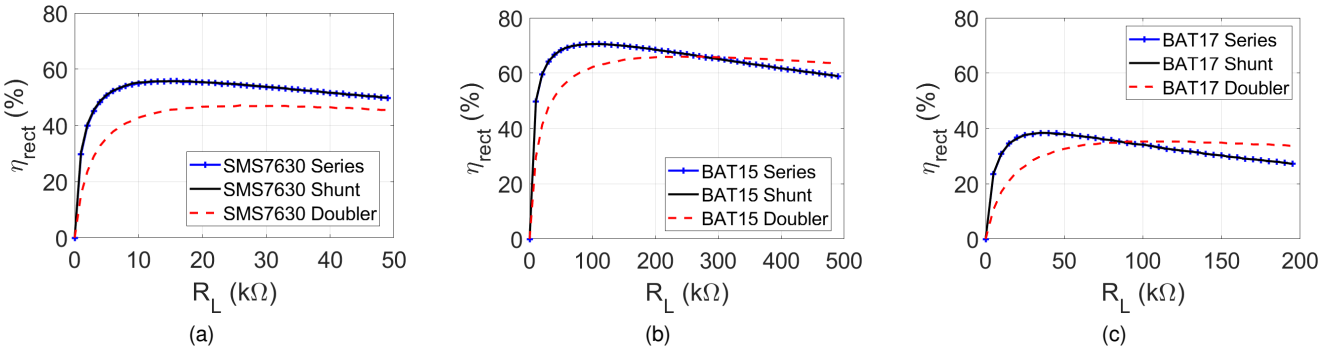

Fig. 1. Simulated RF-to-DC conversion efficiency, η_{rect}, as a function of the load for different rectifier topologies implemented with three Schottky diodes. The working frequency is 889 MHz and the input RF power -20 dBm. (a) Diode SMS7630, (b) diode BAT-15 and (c) diode BAT-17.

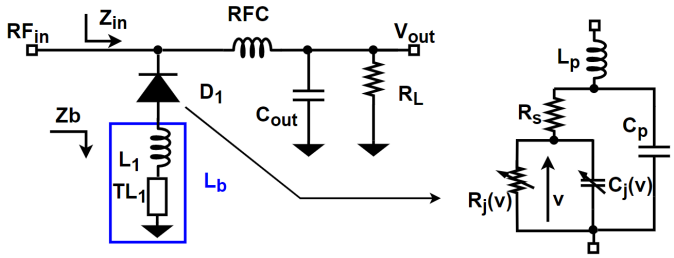

Fig. 2. Schematic of the low input power rectifier using the inductive matching technique.

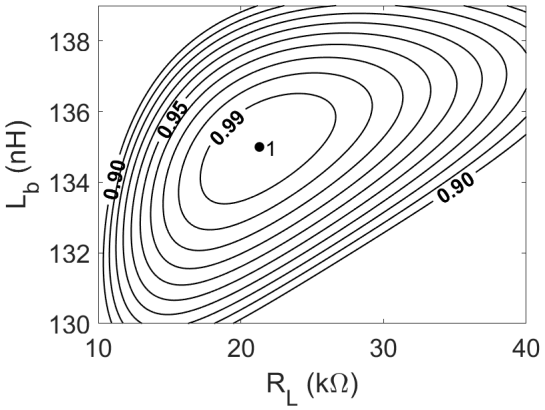

Fig. 3. Simulated contours of the normalized efficiency η_T of the proposed rectifier as function of L_b and R_L. The input RF power is -20 dBm.

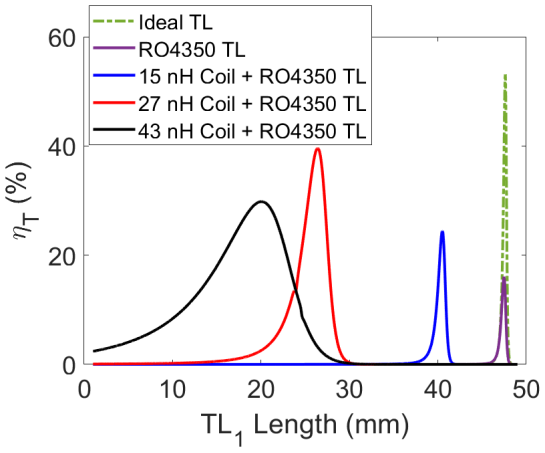

Fig. 4. Simulated rectifier efficiency η_T as a function of TL_1 for different combinations of L_1 and TL_1. The input RF power is -20 dBm.

At a specific input RF power and frequency, from (1) and (2), it can be seen that Z_{in} can be controlled with L_b and the load R_L. The latter has a direct impact in $R_j(v)$ and $C_j(v)$ since the DC voltage at R_L is also the reverse bias voltage of the diode. While the dependency on the load with respect to Z_{in} and η_{rect} is widely discussed in the literature, finding a compromise value of the load to both increase η_{rect} and to achieve efficient impedance matching was not highlighted. This optimization is performed through the inductive technique and the impedance matching is performed with respect to a $50\,\Omega$ source.

For an input RF power of -20 dBm, Fig. 3 presents the simulated total efficiency, η_T, normalized with respect to the maximal efficiency obtained with this technique for different R_L and L_b values. A non-normalized maximal efficiency of $57\,\%$ is obtained at $R_L = 21\,k\Omega$ and $L_b = 135$ nH when resistive loss is not considered in L_b. For 889 MHz and -20 dBm, the value of $R_L = 21\,k\Omega$ becomes the rectifier optimal load for η_T which is different to the optimal load for η_{rect}.

In practice, the value of $L_b = 135$ nH in Fig. 2 can be achieved with a lumped inductor, L_1, a shorted transmission line, TL_1, or a combination of both. At -20 dBm, Fig. 4 shows the rectifier performance obtained when considering loss in L_b and different values of L_1 and TL_1 lengths. As expected, the highest efficiency is obtained with an ideal lossless TL_1.

When considering real substrates, η_T is reduced. Here a 0.7 mm-thick Rogers RO4350 substrate is considered. When only using a TL_1, the efficiency is considerably decreased due to the loss of a long transmission line. A high Q-factor coil, L_1, may be used instead of TL_1. However, coils with high inductance values have a reduced Q-factor decreasing η_T. As a result, the value of the inductive branch L_b is achieved with a combination of TL_1 and L_1. The value of each component in L_b is selected making a trade-off in terms of losses each component introduces. Therefore, an optimized combination is employed in this design. L_b is achieved with a high Q 2712sp-27N Coilcraft inductor and a 26.4 mm shorted stub, TL_1.

In the manufactured RF rectifier, an RF choke of 400 nH is used to block the fundamental and harmonic frequencies from

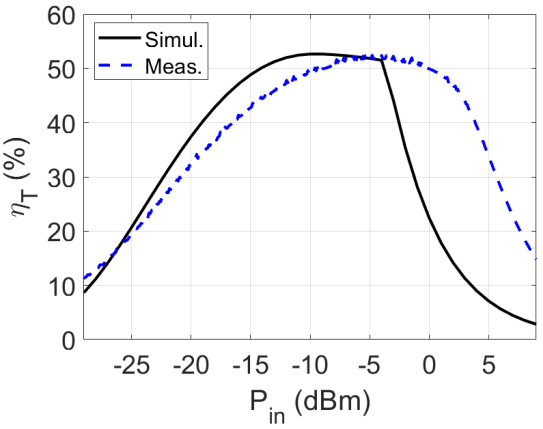

Fig. 5. Simulation and measured efficiencies, η_T, obtained for the low input power rectifier using the inductive matching technique.

the load, and a 1 nF capacitor, C_{out}, is used for smoothing the output DC voltage of the rectifier.

Using a Rohde & Schwarz (R&S) ZVA 50 vector network analyser, a measured reflection coefficient of -28 dB is obtained at 888.7 MHz. For measuring η_T, the rectifier is fed with an 888.7-MHz continuous wave (CW) signal using an R&S SMBV 100 vector signal generator. The DC voltage is measured at the output of the rectifier using a Keithley 195 DC meter when the rectifier is loaded with a 11 kΩ resistor, which at -20 dBm, is the experimental optimal load found as explained in Section II-B.

Fig. 5 shows the simulation and experimental results. An efficiency η_T of 32 % and an output voltage V_{load} of 186 mV are obtained for an input power of -20 dBm. The peak efficiency is 52 % at -4 dBm which corresponds to an output voltage of 1.5 V. At -29 dBm the rectifier has an efficiency of 11 % and an output voltage of 40 mV. Differences between measurement and simulation are remarked due to uncertainties introduced by the tolerance values of the lumped inductor as well as the diode model, *e.g.* the breakdown voltage, V_b, observed in Fig. 5.

At -20 dBm, a relatively high DC output voltage is obtained while reaching good efficiencies.

B. RF rectifier and PMIC interface considerations

Because of its low quiescent current, the commercial BQ25570 PMIC from TI is chosen. To study the characteristics of a rectifier connected with the PMIC, at a specific frequency and operating power, the rectifier is modeled at its output as a voltage source with an internal resistor, R_{int}, as in [26]. R_{int} models the output impedance of the rectifier, which is also the rectifier optimal load for η_T.

This model is used in [12] to measure the impact of R_{int} on the minimal input power and voltage required by the PMIC to output a regulated DC voltage and powers of hundreds of nW. The authors show that R_{int} in the model must be higher than 10 kΩ to limit the quiescent power of the PMIC. Loads higher than 10 kΩ do not substantially reduce the power the PMIC absorbs. The rectifier in Section II-A was designed with an optimal load higher than 10 kΩ, and therefore, it is suitable for the operation of the PMIC at low powers.

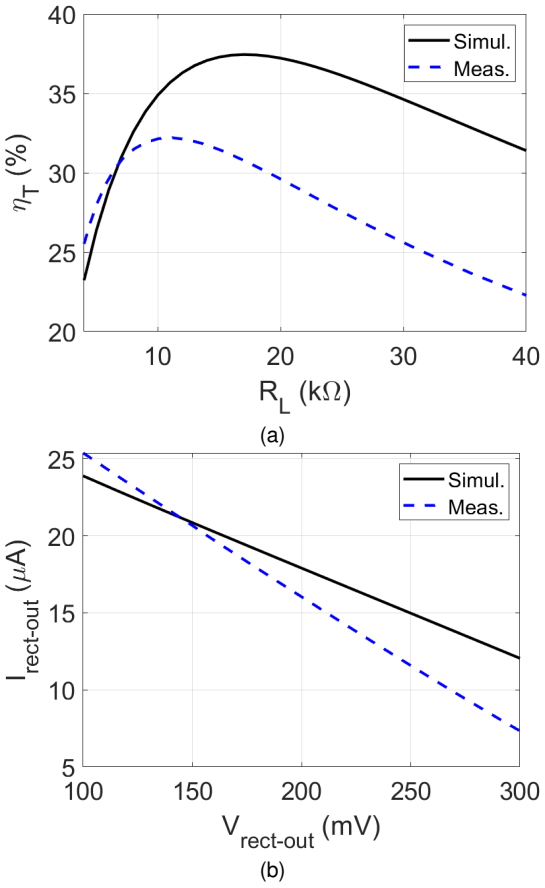

Fig. 6. Simulated and measured results of the designed rectifier. (a) Optimal load and (b) I-V characteristic.

Using a Yokogawa GS610 source measurement unit, the load of the rectifier designed in Section II-A is varied at an input power of -20 dBm and at 888.7 MHz to find the optimal experimental load at this operating point, as shown in Fig. 6(a). Fig. 6(b) presents the measured I-V characteristic of the designed rectifier. Indeed, this characteristic corresponds to a voltage source in series with its internal resistor, whose equation is:

$$I_{meas} = -0.09 \cdot V_{meas} + 34.2, \tag{3}$$

where I_{meas} and V_{meas} are the measured output current in μA and output voltage in mV, respectively.

The inverse of the slope is the experimental optimal load found in Fig. 6(a) and corresponds approximately to 11 kΩ.

Finally, the rectifier is connected to a BQ25570 PMIC. The latter uses a fractional MPPT algorithm to load its source with its optimal load. This algorithm consists of sampling and presenting to the source a fraction of its open-circuit voltage V_{oc}. The most appropriate fraction can be settled depending on the source being used. To determine the most appropriate V_{oc} fraction for the designed rectifier, from (3), a rectifier V_{oc} of 378 mV is obtained when making I_{meas} equal to 0. Half of this open-circuit voltage is 189 mV, which is the voltage that the rectifier delivers at its optimal load. Consequently, the MPPT of the BQ25570 is fixed to 50 %.

TABLE I
COMPARISON OF LOW INPUT POWER RF ENERGY HARVESTERS OPERATING AT SUB-GHZ FREQUENCIES

Ref.	Freq.	Technology	Waveform	PMIC	Regulation[1]	Sensitivity[2] (S)	η_T @-20 dBm
[7]	450 MHz	SMS7630	Chaotic	-	-	-	38 %
[29]	868 MHz	HSMS285C	CW	-	-	-	28 %
[27]	858 MHz	SMS7630	CW	-	-	-	43 %
[30]	935 MHz	HSMS285C	CW	BQ25570	Yes	-15.1 dBm	20 %
[31] [32]	868 MHz	SMS7630	CW	AEM30940	Yes	-15 dBm	21 %
[28] [33]	868 MHz	130-nm CMOS	CW	In-house VCR[3]	Yes	-24.3 dBm	46 %
This work/ [21]	889 MHz	BAT15	CW	BQ25570	Yes	-20 dBm	32 %

[1]Regulation of the output DC voltage.

[2]Minimal input power to keep the PMIC operating.

[3]Voltage current reference.

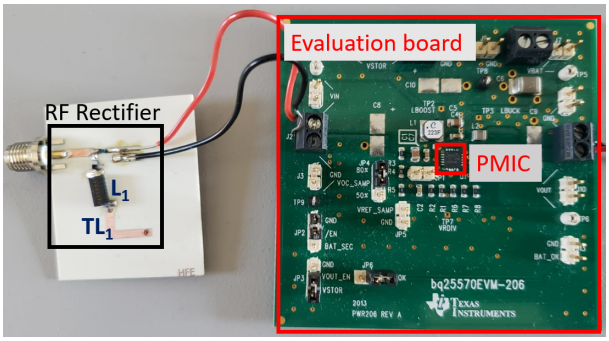

Fig. 7. Photograph of the fabricated low power RF rectifier connected to a BQ25570 PMIC.

The fabricated low input power RF rectifier, along with the PMIC, is shown in Fig. 7. The width of the RF rectifier is 1.9 cm (0.055λ) and its length is 2.1 cm (0.061λ).

With an input power of -20 dBm to the rectifier, the PMIC is capable of operating on its normal mode without disabling its load, and hence, providing a continuous regulated voltage of 1.8 V and hundreds of nW.

Table I compares RF rectifiers as well as RF harvesters composed of an RF rectifier and a PMIC operating at low powers. Although high peak-to-average power ratio (PAPR) signals increase η_T, they lead to complex waveform design, reducing the efficiency of power amplifiers on the transmitter side. [27] and [28] achieve a high η_T by using a custom antenna matched to the input impedance of the rectifier and avoid losses in the MN. The custom antenna is designed for both a specific frequency and operating power of the RF rectifier. Extending the dynamic range of the RF harvester adds complexity to the design of an efficient custom antenna matched to a wide dynamic range of the rectifier. Our proposed RF harvester is designed for use with commercial $50\,\Omega$ antennas, providing flexibility in selecting antennas with different gains/beamwidths, according to the application.

III. WIDE POWER RANGE RF HARVESTER

Inspired by the technique presented in Section II-A, two rectifiers are associated in parallel, as depicted in Fig. 8. The inductive matching technique is employed to compensate the

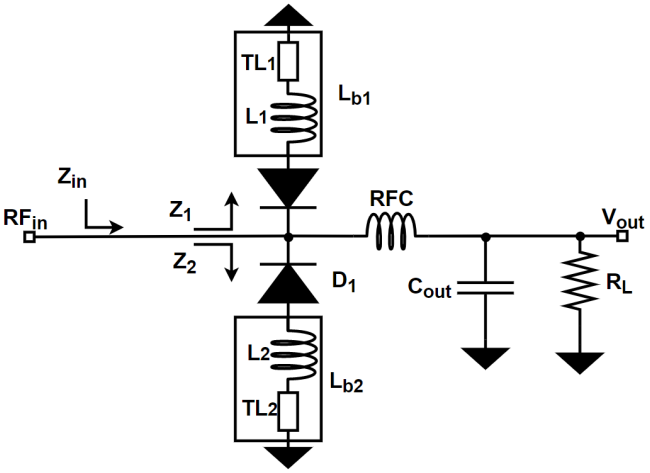

Fig. 8. Parallel association of rectifiers and use of the inductive matching technique in each rectifier.

capacitive behavior of each rectifier diode with the inductive branches L_{b1} et L_{b2}. To keep high efficiencies at low input RF powers, the strategy adopted is to distribute the power only to one rectifier optimized for -20 dBm and to distribute the input RF power among the others as input power increases. This strategy allows losses to be produced only in one diode and only in one inductive branch at low powers. In Section III-A, a study of the behavior of rectifiers as a function of the input RF power level is carried out. Considering the dependency of rectifier parameters, such as input impedance and optimal load, on the input power level, the design of the wide power range RF harvester is detailed in Section III-B. Implementation and measurement details of an association of two rectifiers optimized at -20 dBm and 0 dBm are provided in Section III-C. A discussion over a generalization of our approach to N-rectifiers is carried out in Section III-D by studying a 3-rectifier association.

A. Study of the influence of the input RF power level on rectifiers

Due to the nonlinear nature of the diodes, the optimal load and the input impedance, Z_{in}, of rectifiers are power

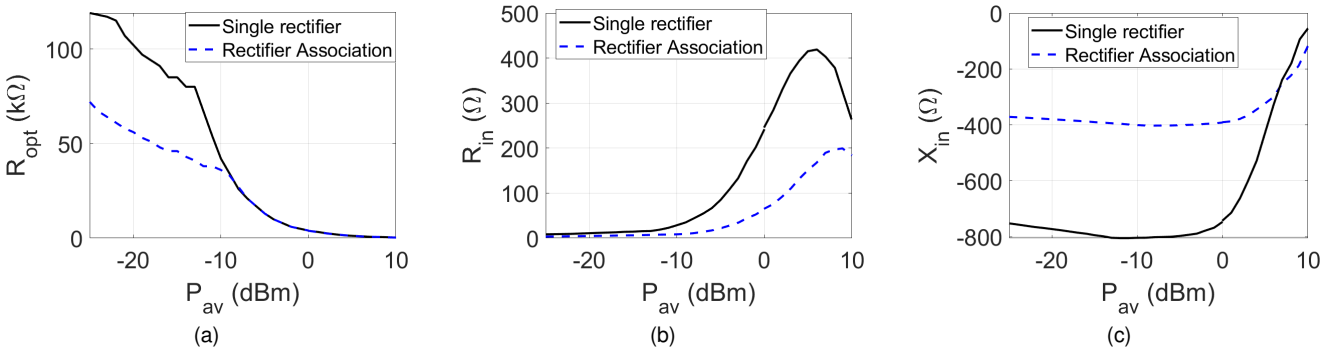

Fig. 9. Dependence of the rectifier parameters on the input RF power obtained in simulation. (a) Optimal load R_{opt}, (b) real part of Z_{in} and (c) imaginary part of Z_{in}.

dependent. For a single rectifier and a parallel association of two rectifiers, Fig. 9 shows the dependence of these parameters on the RF power available, P_{av}, at the input of the diodes, *i.e.*, the power going into the diodes after any reflections. To analyze the variation of these parameters without the influence of a MN, the inductive branches are not considered. Moreover, Z_{in} is obtained when the rectifiers are loaded with their optimal loads R_L at each power level. Simulation results are obtained using ADS Keysight software.

From Fig. 9(a), it can be seen that the optimal load of a rectifier decreases as the available RF power increases. This behavior is justified with the equation of the junction resistance $R_j(v)$ of a Schottky diode:

$$R_j(v) = \frac{V_T}{I_s + i_d(v)}, \tag{4}$$

where V_T is the thermal voltage, I_s is the reverse current and $i_d(v)$ is the diode conduction current. Effectively, higher input RF powers imply higher i_d through the diode reducing R_j. The optimal load of an RF rectifier must be 1.3 to 1.4 times the diode intrinsic resistor [6].

The behavior change in Fig. 9(a) is observed when the rectifiers reach their saturation DC voltage which corresponds to half of V_b. As the load decreases, the saturation voltage is reached at higher P_{av}.

When considering only the junction resistive and capacitive effects of a diode, the input impedance of a rectifier can be expressed as:

$$Z_{in} = \frac{R_j(v)}{1 + [R_j(v)C_j(v)\omega]^2} - j\frac{R_j(v)^2 C_j(v)\omega}{1 + [R_j(v)C_j(v)\omega]^2}. \tag{5}$$

Considering the classical equation of the diode junction capacitive effect, $C_j(v)$ is a decreasing function of the voltage v (*i.e.* of the P_{av}). The variation of $R_j(v)$ and $C_j(v)$ explains the behavior of Z_{in} in the simulation results depicted by Fig. 9(b) and Fig. 9(c) for a BAT15 diode. Regarding X_{in}, for P_{av} higher than 0 dBm and a fixed frequency of 889 MHz, $R_j(v)$ is low and as P_{av} increases, $C_j(v)$ decreases, which leads to a decrease of $|X_{in}|$. For a single rectifier, obtained X_{in} calculations are $-422\,\Omega$ and $-48\,\Omega$ at 5 dBm and 10 dBm, respectively. It has been considered that $R_j(v)$ has values around $1\,\text{k}\Omega$ and $300\,\Omega$ at these power levels, respectively, and that for powers higher than 0 dBm, the DC voltage across the diode is close to $V_b/2$. The calculated values are close to the simulated ones which are $-430\,\Omega$ and $-56\,\Omega$, respectively. Calculated values serve as a good initial approximation; however, simulation results offer a greater accuracy.

The variation of the optimal load and Z_{in}, as a function of the input RF power level, are considered in the design of the wide RF harvester, as described in the following section.

B. Wide power range RF harvester design

As input power varies, loading the rectifiers with their optimal load is achieved with the MPPT algorithm of the PMIC as described in Section II-B. Power distribution is achieved with the values of the inductive branches by matching the input impedance of each rectifier to a $50\,\Omega$ RF source based on the input RF power level. The matching is mainly achieved by eliminating the imaginary part of Z_i with L_{bi} as depicted in Fig. 8. For an association of two rectifiers, Fig. 10 shows the total efficiencies, η_T, normalized with respect to the maximum efficiencies obtained at -20 dBm and 0 dBm respectively. η_T varies based on L_{b1} and L_{b2}. Ohmic losses in the inductive branches are included in the results to consider losses at low powers. At -20 dBm, the maximal efficiency is reached when one branch is 130 nH while the other branch must have a value different from 130 nH. This indicates that one branch is well-matched, whereas the other is mismatched. Effectively, 130 nH is near the value found in Section II-A, meaning only one rectifier is operating. Moreover, to achieve an acceptable impedance matching while limiting the losses in the complex MN, the input impedance of this branch is optimized making a trade-off between L_{b1} and R_L as described in Section II-A.

At 0 dBm, the maximal efficiency is achieved when L_{b1} and L_{b2} are equal and have a value of 133 nH. Furthermore, from Fig. 9(a), it can be seen that R_{in} of the association at this power of operation is already close to $50\,\Omega$, meaning that a trade-off between the inductive branches and R_L is not required after compensating the imaginary part of the diodes. The close value of the optimal inductive branch at -20 dBm with the values of the inductive branches at 0 dBm is explained by the negligible variation of X_{in} from -20 dBm to 0 dBm as depicted in Fig. 9(c). Although a maximal efficiency at -20 dBm means a different value of one of the inductive branches, a trade-off between L_{b1} and L_{b2} allowing high

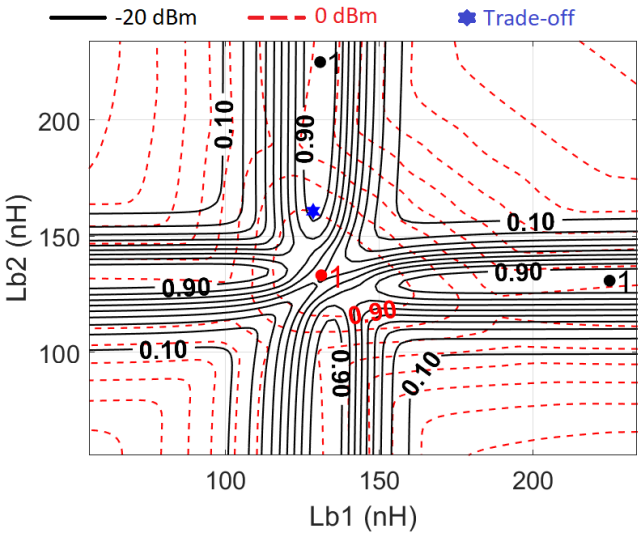

Fig. 10. Evaluation of L_{b1} and L_{b2} to obtain high efficiencies at -20 dBm and 0 dBm. Contours indicate normalized simulated efficiencies η_T.

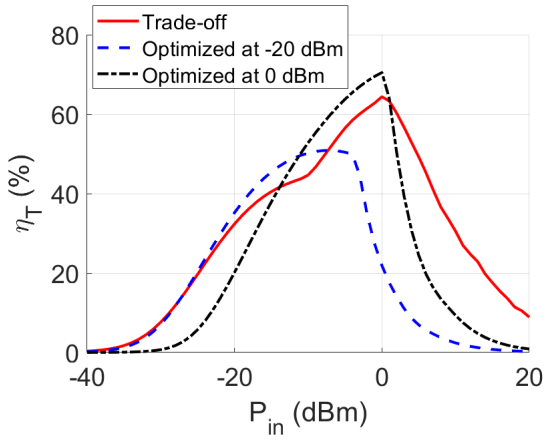

Fig. 11. Simulated efficiency comparison of a rectifier optimized at -20 dBm, 0 dBm and the rectifier association optimized at -20 dBm and 0 dBm.

efficiencies at both power levels can be found as showed in Fig. 10.

In simulation, Fig. 11 shows η_T comparison of a rectifier optimized at -20 dBm, 0 dBm and the rectifier association optimized at -20 dBm and 0 dBm. For the latter, η_T of 33 % and 64 % are achieved at -20 dBm and 0 dBm for optimal loads of 17 kΩ and 4 kΩ, respectively. The loss in terms of η_T at each power level is small and justified by the efficient increase of the RF harvesting range. Fig. 12 shows the power distribution in each rectifier of the association designed for an efficient operation between -20 dBm and 0 dBm. As it can be observed, at -20 dBm the power is mainly distributed to the rectifier intended for this power level, limiting losses only to one branch. At 0 dBm, the input power is distributed between both rectifiers.

In Fig. 9(c), from 0 dBm to higher powers, the capacitive behavior of a diode decreases, leading to lower inductive branch values. Effectively, to increase the range of the RF harvester for powers higher than 0 dBm while keeping high

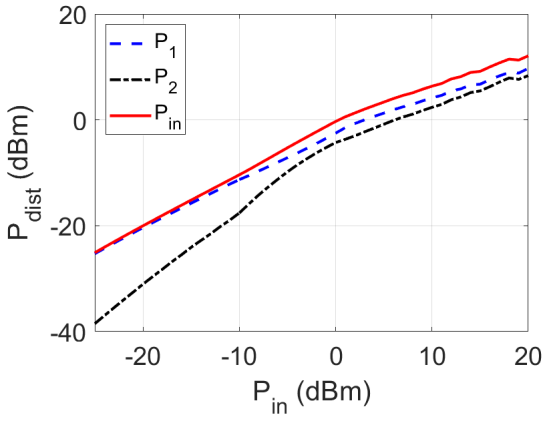

Fig. 12. Simulated power distribution between the branches of the rectifier association optimised for an efficient operation between -20 dBm and 0 dBm.

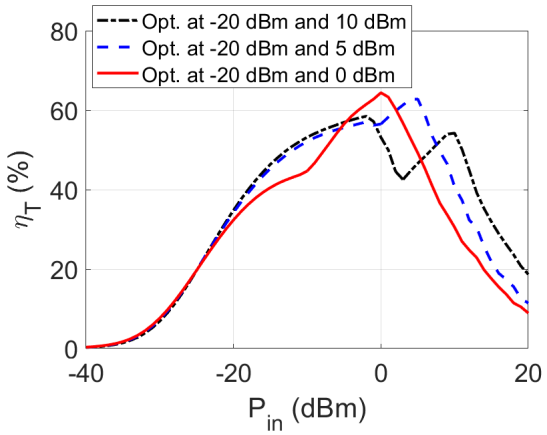

Fig. 13. Simulated RF power range increment as L_{b2} is varied in a two-diode rectifier association using the BAT15 diode

efficiencies at low powers, the value of one inductive branch is reduced while the other is kept at the optimal inductive branch value found at -20 dBm. Fig. 13 shows how the RF power range is increased as the value of one of the inductive branches is varied. As power increases, the trade-off done between L_{b1} and L_{b2} is no longer necessary. The values of L_{b2} corresponding to the optimizations at 0 dBm, 5 dBm and 10 dBm are 161 nH, 91 nH and 44 nH respectively. For powers higher than 0 dBm, the efficiency is mainly a contribution of the rectifier optimized for high power levels contrary to 0 dBm where both rectifiers contribute to the output power.

Here, an association of two rectifiers is fabricated at -20 dBm and 0 dBm as described in the following section.

C. Implementation and measurements

Considering the above theoretical and simulation results, an association of two rectifiers optimized at -20 dBm and 0 dBm is designed and manufactured. A photograph of the wide power range RF rectifier is given in Fig. 14. The width of the rectifier association is 2.19 cm (0.063λ) and its length is 4.64 cm (0.13λ).

Measurements are made when the rectifier association is loaded with 12 kΩ and 4 kΩ, which are the experimental optimal loads found at -20 dBm and 0 dBm, respectively. In

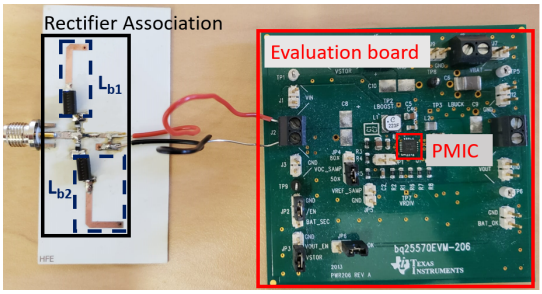

Fig. 14. Fabricated wide power range RF harvester.

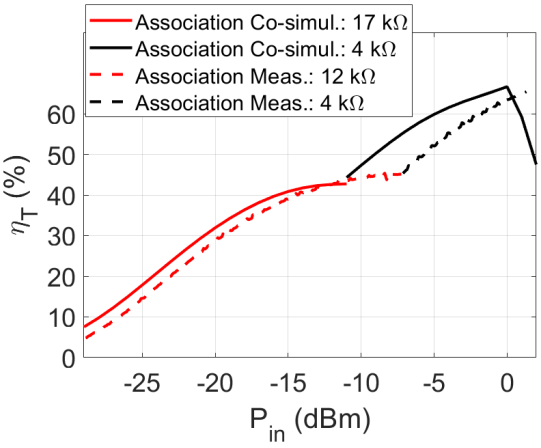

Fig. 15. Simulation and measured results of the association.

the real application, the PMIC with MPPT will present the optimal load of the rectifier at each power level. Fig. 15 shows the simulation and experimental efficiencies. η_T of 29 % and 63 % are obtained at -20 dBm and 0 dBm, respectively.

With an input power of -20 dBm at the association, the PMIC is capable of operating in its normal mode without disabling its load, and hence, providing a continuous regulated DC voltage of 1.8 V and hundreds of nW. TThe design efficiently extends the power harvesting range capabilities while keeping high efficiencies at low powers.

Table II compares the obtained results with similar works found in the literature. At -20 dBm, the present work has the higher η_T. Furthermore, our proposed solution is capable of harvesting for a single device and supplying a regulated voltage through the PMIC for powers as low as -20 dBm, which is not addressed in the other works. The proposed wide range RF harvester is optimized for maximal efficiency at 0 dBm, and it has lower dynamic ranges than other solutions. However, as demonstrated in simulations, peak efficiencies at higher power levels and higher dynamic ranges can be obtained by varying the inductive branch values of one of the rectifiers. Additionally, thanks to the use of the inductive technique, the association is compact, while other proposed designs in similar technologies have larger dimensions. CMOS rectifiers are also presented in Table II for purposes of comparison with rectifiers implemented on other technologies. Although high η_{rect} are reported at low powers, the MN decreases considerably η_T or η_T is not reported. In [12], high η_T is obtained in simulation. However, only losses in diodes were considered to prove the

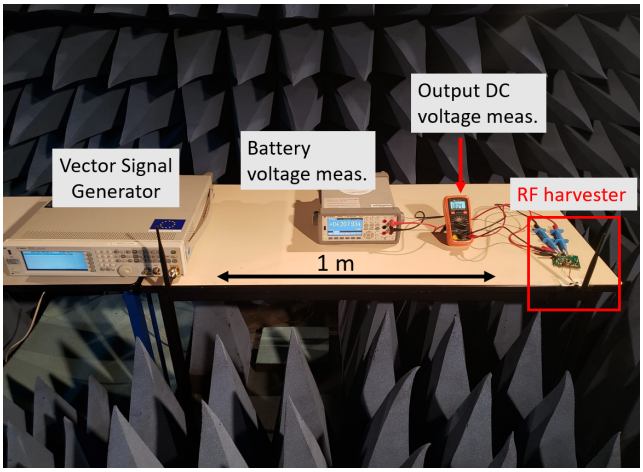

Fig. 16. Setup in an anechoic chamber for wireless power transfer measurements.

circulator concept. Losses in the latter, as well as in the MN, will decrease η_T under the performance obtained in the present work.

Measurements for Wireless Power Transfer (WPT) are carried out in an anechoic chamber as depicted in Fig. 16. The distance between the transmitting and receiving antennas is fixed to 1 meter. The power of the transmitter, P_{trans}, is varied from 13 dBm to 35 dBm. Two commercial antennas are used at the transmitter and receiver side with a gain of approximately 1 dBi at the operation frequency. The real power received by the RF harvester is measured with the Rigol's DSA1030A Spectrum Analyzer. The RF harvester provides a power of 324 nW at a regulated DC voltage of 1.8 V for a transmitted power starting at 13 dBm, which corresponds to a measured received power P_r of -20.3 dBm. When P_{trans} is higher than 13 dBm, the PMIC stores the excess of received energy in a ceramic capacitor. Fig. 17 shows the time required to charge a ceramic capacitor of 100 μF from 2.5 V to 4.2 V as a function of P_r. At P_r of -18 dBm and 2 dBm, the capacitor is charged in 390 s and 1 s, respectively. Estimated charging times are also provided considering simulated η_T of the RF rectifier association and efficiencies of the PMIC provided by the manufacturer at different power levels. The performance of the RF part is not degraded while considering the whole system.

D. Discussion over a 3-rectifier association

Depending on the application, the dynamic range can be extended to higher input RF power levels. For the rectifier operating at high power levels, diodes with higher V_b may be considered to increase the maximal allowed voltage and, therefore, increase the efficiency at high powers. Furthermore, more rectifiers can be associated in parallel to achieve high efficiencies at several specific input power levels. Fig. 18 presents the simulation results for an extension of the dynamic range when using a BAT15 diode with low V_{th} for low and medium powers and a BAT17 diode with a high V_b for higher RF power levels in an association of two and three rectifiers. For example, based on the same approach, simulations results

TABLE II
COMPARISON OF WIDE POWER RANGE RF HARVESTERS

Ref.	[12][1]	[13]	[17]	[20]	[34]	[35]	**This work**
Freq.	868 MHz	2.45 GHz	915 MHz	900 MHz	900 MHz	433 MHz	889 MHz
Technology	4x Schottky diodes	2x Schottky diodes	4x Schottky diodes	3x Schottky diodes	65-nm CMOS	65-nm CMOS	2x Schottky diodes
Method	Use of a circulator	Use of a circulator	Automatic Z_{in} transf.	Adaptive power distribution	Dual Path FX Topo.	DM feedback circuit	Inductive technique
Number of Rectifiers	2	2	2	3	2	4	2
Matching Network	Lump. Comp. L-Topo.	Lump. Comp. Dist. Tech.	T-junction Dist. Tech.	Dist. Tech	Off-chip inductors	None	Inductive branch
Load Type	PMIC	A load per rectifier	A load per rectifier	Constant voltage load	Single Load	Single Load	PMIC
η_T at -20 dBm	43 %	27 %	18 %	0 %	32 % (-16.5 dBm)	86 % (η_{rect})	29 %
η_T at 0 dBm	76 %	20 %	48 %	52 %	-	-	63 %
η_T (Peak)	76 % at 0 dBm	70 % at 12 dBm	67 % at 29 dBm	57.3 % at 15 dBm	35 % at -10 dBm	86 % (η_{rect})	63 % at 0 dBm
Dynamic range	26 dB ($\eta_T > 40$ %)	30 dB ($\eta_T > 40$ %)	28 dB ($\eta_T > 50$ %)	26 dB ($\eta_T > 50$ %)	11 dB ($\eta_T > 20$ %)	10.1 dB ($\eta_{rect} > 80$ %)	20 dB ($\eta_T > 40$ %)
Size (mm^2)	-	80x78 (0.65x0.64)λ	-	$> 100^2$ (0.3x0.3)λ	0.25x0.16 (7.5x4.8)$10^{-4}\lambda$	6480 μm^2	21.9x46.4 (0.065x0.14)λ

[1]Measurement results are not reported, only simulations.

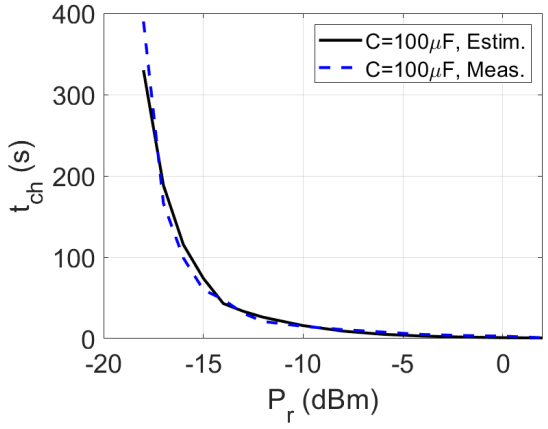

Fig. 17. Estimated and measured required time to charge a 100 μF ceramic capacitor with energy harvested from a distant RF power source.

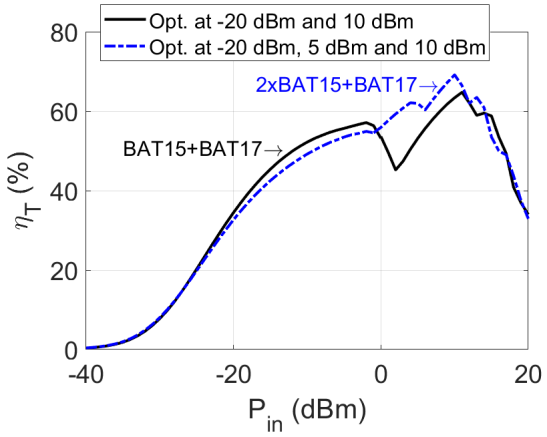

Fig. 18. Simulated RF power range increment in associations of two and three rectifiers using different diodes.

revealed that the association of three rectifiers presents η_T of 32 %, 62 % and 69 % at power levels of -20 dBm, 5 dBm and 10 dBm for optimal loads of 15 kΩ, 800 Ω and 200 Ω, respectively.

As the input RF power increases, the output DC voltage also increases. Since for low input powers, the chosen diodes have low V_{th} and C_{j0}, leading to low V_b, particularly attention must be paid when increasing power with other diodes and branches. High output DC voltages may result in leakage currents or damage to low power V_b diodes.

IV. CONCLUSION

A wide range RF energy harvester is demonstrated in this paper while keeping good efficiencies at low powers. Firstly, an efficient low input power RF rectifier is designed with the inductive technique. Measured efficiency of 32 % and a DC voltage of 186 mV are achieved at an input power of -20 dBm and a frequency of 888.7 MHz.

Afterwards, the efficient low input power RF rectifier is associated with a second rectifier that extends the RF harvesting range. Measured efficiencies of 29 % and 63 % are

obtained at -20 dBm and 0 dBm, respectively, demonstrating the wide RF harvesting range while keeping high efficiencies at low power levels. At -20 dBm, the association is capable of maintaining the operation of a commercial PMIC that regulates the DC output voltage of the rectifier and delivers hundreds of nW aiming to power ultralow power devices. The harvester is fabricated with off-the-shelf components and high efficiencies are obtained using a CW signal.

REFERENCES

[1] F. Ait Aoudia, M. Gautier, M. Magno, O. Berder, and L. Benini, "Leveraging energy harvesting and wake-up receivers for long-term wireless sensor networks," *Sensors*, vol. 18, no. 5, p. 1578, 2018.

[2] H. Rahmani, D. Shetty, M. Wagih, Y. Ghasempour, V. Palazzi, N. B. Carvalho, R. Correia, A. Costanzo, D. Vital, F. Alimenti, J. Kettle, D. Masotti, P. Mezzanotte, L. Roselli, and J. Grosinger, "Next-Generation IoT Devices: Sustainable Eco-Friendly Manufacturing, Energy Harvesting, and Wireless Connectivity," *IEEE Journal of Microwaves*, vol. 3, no. 1, pp. 237–255, 2023.

[3] Z. Jouni, T. Soupizet, S. Wang, A. Benlarbi-Delai, and P. M. Ferreira, "1.2 nW Neuromorphic Enhanced Wake-Up Radio," in *SBC/SBMicro/IEEE/ACM Symposium on Integrated Circuits and Systems Design (SBCCI)*, 2022, pp. 1–6.

[4] S. Oh, N. E. Roberts, and D. D. Wentzloff, "A 116 nW multi-band wake-up receiver with 31-bit correlator and interference rejection," in *IEEE Custom Integrated Circuits Conference (CICC)*, 2013, pp. 1–4.

[5] K. Kotani, A. Sasaki, and T. Ito, "High-Efficiency Differential-Drive CMOS Rectifier for UHF RFIDs," *IEEE Journal of Solid-State Circuits*, vol. 44, no. 11, pp. 3011–3018, 2009.

[6] C. R. Valenta and G. D. Durgin, "Harvesting Wireless Power: Survey of Energy-Harvester Conversion Efficiency in Far-Field, Wireless Power Transfer Systems," *IEEE Microwave Magazine*, vol. 15, no. 4, pp. 108–120, 2014.

[7] A. Collado and A. Georgiadis, "Improving wireless power transmission efficiency using chaotic waveforms," in *IEEE/MTT-S International Microwave Symposium Digest*, 2012, pp. 1–3.

[8] M. Gonzalez, P. Xu, R. Dekimpe, M. Schramme, I. Stupia, T. Pirson, and D. Bol, "Technical and Ecological Limits of 2.45-GHz Wireless Power Transfer for Battery-Less Sensors," *IEEE Internet of Things Journal*, vol. 10, no. 17, pp. 15 431–15 442, 2023.

[9] A. Litvinenko, J. Eidaks, and A. Aboltins, "Usage of Signals with a High PAPR Level for Efficient Wireless Power Transfer," in *2018 IEEE 6th Workshop on Advances in Information, Electronic and Electrical Engineering (AIEEE)*, 2018, pp. 1–5.

[10] Y. Huang, N. Shinohara, and T. Mitani, "Impedance Matching in Wireless Power Transfer," *IEEE Transactions on Microwave Theory and Techniques*, vol. 65, no. 2, pp. 582–590, 2017.

[11] K. R. Sadagopan, J. Kang, Y. Ramadass, and A. Natarajan, "A cm-Scale 2.4-GHz Wireless Energy Harvester With NanoWatt Boost Converter and Antenna-Rectifier Resonance for WiFi Powering of Sensor Nodes," *IEEE Journal of Solid-State Circuits*, vol. 53, no. 12, pp. 3396–3406, 2018.

[12] J. Argote-Aguilar, F.-D. Hutu, G. Villemaud, M. Gautier, and O. Berder, "Efficient Association of Low and High RF Power Rectifiers for Powering Ultra-Low Power Devices," in *IEEE International Conference on Electronics, Circuits and Systems (ICECS)*, 2022, pp. 1–4.

[13] H. Zhang, Y.-x. Guo, Z. Zhong, and W. Wu, "Cooperative Integration of RF Energy Harvesting and Dedicated WPT for Wireless Sensor Networks," *IEEE Microwave and Wireless Components Letters*, vol. 29, no. 4, pp. 291–293, 2019.

[14] H. Sun, Z. Zhong, and Y.-X. Guo, "An Adaptive Reconfigurable Rectifier for Wireless Power Transmission," *IEEE Microwave and Wireless Components Letters*, vol. 23, no. 9, pp. 492–494, 2013.

[15] S. Y. Zheng, S. H. Wang, K. W. Leung, W. S. Chan, and M. H. Xia, "A High-Efficiency Rectifier With Ultra-Wide Input Power Range Based on Cooperative Structure," *IEEE Transactions on Microwave Theory and Techniques*, vol. 67, no. 11, pp. 4524–4533, 2019.

[16] P. Wu, Y.-d. Chen, W. Zhou, Z. H. Ren, and S. Y. Huang, "A Wide Dynamic Range Rectifier Array Based on Automatic Input Power Distribution Technique," *IEEE Microwave and Wireless Components Letters*, vol. 30, no. 4, pp. 437–440, 2020.

[17] M. Huang, Y. L. Lin, J.-H. Ou, X. y. Zhang, Q. W. Lin, W. Che, and Q. Xue, "Single- and Dual-Band RF Rectifiers with Extended Input Power Range Using Automatic Impedance Transforming," *IEEE Transactions on Microwave Theory and Techniques*, vol. 67, no. 5, pp. 1974–1984, 2019.

[18] Z. He, J. Lan, and C. Liu, "Compact Rectifiers With Ultra-wide Input Power Range Based on Nonlinear Impedance Characteristics of Schottky Diodes," *IEEE Transactions on Power Electronics*, vol. 36, no. 7, pp. 7407–7411, 2021.

[19] S. Trovarello, G. Paolini, D. Masotti, and A. Costanzo, "Cascaded Rectifiers for Energy Harvesting With a Wide Dynamic Power Range," *IEEE Journal of Radio Frequency Identification*, vol. 7, pp. 64–73, 2023.

[20] X. Wang and A. Mortazawi, "Rectifier Array With Adaptive Power Distribution for Wide Dynamic Range RF-DC Conversion," *IEEE Transactions on Microwave Theory and Techniques*, vol. 67, no. 1, pp. 392–401, 2019.

[21] J. Argote-Aguilar, M.-D. Wei, F.-D. Hutu, G. Villemaud, M. Gautier, O. Berder, and R. Negra, "Low-input-power Sub-GHz RF Energy Harvester for Powering Ultra-low-power Devices," in *International Workshop on Integrated Nonlinear Microwave and Millimetre-Wave Circuits (INMMIC)*, 2023, pp. 1–4.

[22] *Surface-Mount Mixer and Detector Schottky Diodes*, Skyworks, 2021. [Online]. Available: https://www.skyworksinc.com/-/media/SkyWorks/Documents/Products/201-300/Surface_Mount_Schottky_Diodes_200041AG.pdf

[23] *Single silicon RF Schottky diode*, Infineon, 2018. [Online]. Available: https://https://www.infineon.com/dgdl/Infineon-BAT15-03W-DS-v01_00-EN.pdf

[24] *Silicon Schottky Diode*, Infineon, 2007. [Online]. Available: https://www.infineon.com/dgdl/Infineon-BAT17-DataSheet-v01_00-EN.pdf

[25] M.-D. Wei, C.-Y. Fan, F. Dietrich, and R. Negra, "General Solution of a Rectifier Using an Inductive Matching Network," *IEEE Microwave and Wireless Components Letters*, vol. 30, no. 12, pp. 1173–1176, 2020.

[26] S.-E. Adami, V. Marian, N. Degrenne, C. Vollaire, B. Allard, and F. Costa, "Self-powered ultra-low power DC-DC converter for RF energy harvesting," in *IEEE Faible Tension Faible Consommation*, 2012, pp. 1–4.

[27] M. Wagih, A. S. Weddell, and S. Beeby, "High-Efficiency Sub-1 GHz Flexible Compact Rectenna based on Parametric Antenna-Rectifier Co-Design," in *IEEE/MTT-S International Microwave Symposium (IMS)*, 2020, pp. 1066–1069.

[28] D. Shetty, C. Steffan, G. Holweg, W. Bösch, and J. Grosinger, "Submicrowatt CMOS Rectifier for a Fully Passive Wake-Up Receiver," *IEEE Transactions on Microwave Theory and Techniques*, vol. 69, no. 11, pp. 4803–4812, 2021.

[29] S. D. Assimonis, S.-N. Daskalakis, and A. Bletsas, "Sensitive and Efficient RF Harvesting Supply for Batteryless Backscatter Sensor Networks," *IEEE Transactions on Microwave Theory and Techniques*, vol. 64, no. 4, pp. 1327–1338, 2016.

[30] N. John, F. Ludivine, and T. Thierry, "An RF-Powered IoT Node for Environment Sensoring," in *IEEE Wireless Power Transfer Conference (WPTC)*, 2019, pp. 301–306.

[31] A. Sidibe and A. Takacs, "Compact 3D Rectenna for Low-Power Wireless Transmission," in *General Assembly and Scientific Symposium of the International Union of Radio Science (URSI GASS)*, 2021, pp. 1–4.

[32] A. Sidibe, G. Loubet, A. Takacs, and D. Dragomirescu, "A multifunctional battery-free bluetooth low energy wireless sensor node remotely powered by electromagnetic wireless power transfer in far-field," *Sensors*, vol. 22, no. 11, p. 4054, 2022.

[33] D. Shetty, C. Steffan, G. Holweg, W. Bösch, and J. Grosinger, "Ultra-Low-Power Sub-1 V 29 ppm/°C Voltage Reference and Shared-Resistive Current Reference," *IEEE Transactions on Circuits and Systems I: Regular Papers*, vol. 70, no. 3, pp. 1030–1042, 2023.

[34] Y. Lu, H. Dai, M. Huang, M.-K. Law, S.-W. Sin, S.-P. U, and R. P. Martins, "A Wide Input Range Dual-Path CMOS Rectifier for RF Energy Harvesting," *IEEE Transactions on Circuits and Systems II: Express Briefs*, vol. 64, no. 2, pp. 166–170, 2017.

[35] A. S. Almansouri, J. Kosel, and K. N. Salama, "A Dual-Mode Nested Rectifier for Ambient Wireless Powering in CMOS Technology," *IEEE Transactions on Microwave Theory and Techniques*, vol. 68, no. 5, pp. 1754–1762, 2020.

Jesus Argote (Graduate Student Member, IEEE) received the master's degree in electrical engineering from the National Institute of Applied Sciences of Lyon in 2021. He is currently pursuing the Ph.D. degree with the IRISA Laboratory, University of Rennes and in co-direction with the CITI Laboratory, Institute of Applied Sciences of Lyon. He was a visitor Ph.D student in the HFE laboratory, RWTH Aachen University in 2023. His graduate research focuses on ultralow-power wake-up radios and radio frequency energy harvesting.

Muh-Dey Wei received his M.Sc. and Ph.D. degree from National Chung Cheng University, Taiwan, in electrical engineering in 2006 and 2011, respectively. During his Ph.D. he spent 18 months with Mixed Signal CMOS Circuits (MSCC) and Chair for Integrated Analog Circuits and RF Systems (IAS) at RWTH Aachen University, Aachen, Germany. He is currently a chief engineer at Chair of High Frequency Electronics (HFE), RWTH Aachen University, Aachen, Germany. His current research interests are wireless power transfer, rectifiers, 2D material, advanced transceivers, microwave frequency sources, and power amplifiers.

Dr. Wei is the recipient of a Deutscher Akademischer Austauschdienst (DAAD) Scholarship.

Florin Hutu (IEEE SM. 2020) received the Engineering degree in electronics and telecommunications and the M.Sc. degree in digital radiocommunications from "Gheorghe Asachi" Technical University of Iași, Romania, in 2003 and 2004 respectively. In 2007, he received the Ph.D. degree in automatic control from the University of Poitiers, France. After two years of post-doctorate at XLIM research institute, in September 2010, he became an associate professor at INSA Lyon, France. He joined the INSA Lyon's Electrical Engineering department and the INSA Lyon and INRIA's CITI laboratory. He is the author of more than 90 national and international scientific papers. His research interests include energy-efficient radiocommunications (wake-up radio, energy harvesting and wireless power transfer) and RFID technologies. He is also involved in the design of software-defined radio architectures for the IoT and radio front-end architectures for millimeter wave communications (hybrid beamforming).

Guillaume Villemaud received his PhD degree in electronics from the Univ of Limoges, France (2002). He obtained his HDR (Qualification to supervise research) from INSA Lyon and Univ Lyoné 1 (2013). He worked for CREAPE (2002-03) and joined the CITI Lab, Lyon, in 2003. His research interests are RF architectures and system level simulation, Energy harvesting and Wireless Power Transfer, RFID, Backscatter radio, Full-duplex and Spatial Modulation systems, coverage prediction, radio propagation and measurements, antenna design, antenna diversity and multiple antenna processing (SIMO, MIMO). He was the site leader for the European projects: iPlan (Femtocells) and IMMUNet (IIoT), and multiple national projects, also took part of the development of CorteXlab, French equipment of excellence. He has published more than 120 international technical papers, is a Senior Member of IEEE and an Ass Editor of Annals of Telecoms. He was vice-head of the CITI Lab and is now the team leader of RHODES.

Matthieu Gautier holds the Engineering and M.Sc. degrees in electronics and signal processing engineering from the ENSEA graduate school and a Ph.D. degree from Grenoble-INP in 2006. From 2006 to 2011, he was a research engineer at Orange labs, INRIA and CEA-LETI laboratory. He is currently an Associate Professor at the University of Rennes and the IRISA Laboratory since 2011. His research activities are in the two complementary fields of embedded systems and digital communications for energy efficient communication systems.

Olivier Berder received the M.Sc. and Ph.D. degrees in electrical engineering from the University of Bretagne Occidentale, Brest, in 1999 and 2002, respectively. From 2002 to 2004 he was with the Laboratory for Electronics and Telecommunication Systems (LEST–UMR CNRS 6165), Brest. After a post-doc with the Speech and Sound Technologies and Processes Laboratory in Orange labs, Lannion, France, in March 2005 he joined University of Rennes where he is currently a Professor at IUT Lannion, and the laboratory IRISA in Rennes. He is the leader of GRANIT team and his research interests focus on cooperative techniques and power management for mobile communications and wireless sensor networks. He has co-authored more than 120 peer reviewed papers in international journals or conferences and has participated in numerous collaborative projects founded by either European Union or French National Research Agency.

Renato Negra received the M.Sc. degree in telematics from Graz University of Technology, Graz, Austria, and the Ph.D. degree in electrical engineering from ETH Zurich, Zurich, Switzerland. During his M.Sc. studies he spend one year as an exchange student at the Norwegian University of Science and Technology (NTNU), Trondheim, Norway.

From 1998 to 2000 he was with Alcatel Space Norway AS (now NorSpace AS), Horten, Norway where he was involved in the design and characterisation of space-qualified RF equipment. In 2000 he joined the Laboratory for Electromagnetic Fields and Microwave Electronics at the ETH Zurich. There, his Ph.D. research was focused on power-efficient linear amplification of wireless communication signals. He was a Post-Doctoral Fellow at iRadio Lab, University of Calgary, Canada, working on switching-mode power amplifiers and advanced wireless transmitters from 2006 to 2008. Within the Ultra high speed Mobile Information and Communication (UMIC) Research Centre, RWTH Aachen University, Germany, he was appointed as Assistant Professor for Mixed-Signal CMOS Circuits from June 2008 till December 2013. Since December 2013 he is holding the Chair of High Frequency Electronics at the same university.

His research interests are high frequency circuits and systems in both silicon, III-V and 2D-material technologies. Particular interests include power amplifiers and transmitter architectures.